

ZMP Trajectory from Human Body Locomotion Dynamics Evaluated by Kinect-based Motion Capture System

Igor Danilov, Bulat Gabbasov, Ilya Afanasyev and Evgeni Magid

Intelligent Robotic Systems Laboratory (LIRS), Innopolis University, Universitetskaya 1, Innopolis, 420500, Russia

Keywords: Motion Capture (MoCap), Zero Moment Point (ZMP), Kinect Sensor, Biomechanical Analysis of Human Locomotion, Multi-depth Sensor Video Recording.

Abstract: This article presents the methods of zero moment point (ZMP) trajectory evaluation for human locomotion by processing biomechanical data recorded with Kinect-based motion capture (MoCap) system. Our MoCap system consists of four Kinect 2 sensors, using commercial iPi soft markerless tracking and visualization technology. We apply iPi Mocap Studio software to multi-depth sensor video recordings, acquiring visual and biomechanical human gait data, including linear and angular coordinates, velocities, accelerations and center of mass (CoM) position of each joint. Finally, we compute ZMP and ground projection of the CoM (GCOM) trajectories from human body dynamics in MATLAB by two methods, where human body is treated as (1) a single mass point, and (2) multiple mass points (with following ZMP calculation via inertia tensor). The further objective of our research is to reproduce the human-like gait with Russian biped robot AR-601M.

1 INTRODUCTION

The history of humanoid robotics is directly correlated with the active exoskeletons development. Even though one of the first exoskeleton was created almost 50 years ago, in 1969, under the leadership of Yugoslav scientist Miomir Vukobratovic (Vukobratovic and Juricic, 1969), humanoid robotics related research topics keep attracting significant attention of scientists as humanoid locomotion is still too far from human walking stability and energy efficiency (Larsen and Stoy, 2011).

Both humans and humanoids are underactuated systems with no actuation between a foot and supporting surface (Dasgupta and Nakamura, 1999). In order to develop energy-efficient locomotion algorithms for a humanoid, a human gait analysis should be performed (Asano and Luo, 2008). Taking into account significant differences between a human and a humanoid it is not feasible to apply a human gait directly to a robot (Field et al., 2009). These differences include distinct amount of Degrees of Freedom (DoFs) and skeletons, different mass distribution and CoM position, limited capabilities of humanoids relatively to humans in terms of joint constraints (position, velocity and acceleration). Thus, there is no direct mapping of human relative positions to the robot and kinematic mismatch requires kinematic corrections with

calculating the joint angle trajectories. At the same time to keep locomotion balance an advanced control should be applied to the robot, overcoming problems of underactuation and dynamic mismatch (Dasgupta and Nakamura, 1999; Naksuk et al., 2005).

Nevertheless, a number of research teams reported successful automatic generation of robot walking from human walking data through different mathematical models of locomotion control - analysis of MoCap data of a human locomotion provided certain human locomotion outputs, which were further implemented into robotic bipedal locomotion. Sinnet et al. (Sinnet et al., 2011) introduced canonical human walking functions, which were used to form a linear spring-damper system to estimate human-walking behavior. Chalodhorn et al. (Chalodhorn et al., 2007) described a mapping of a human gait data (obtained from MoCap data) onto a body skeleton, applying inverse kinematics procedure; this was followed by using principal component analysis (PCA) to reduce dimensionality of the joints space, building 3D motion space representation of kinematic postures.

As far as the terms of static (GCOM) and dynamic (ZMP) stabilities (Mrozowski et al., 2007) can be used to biped and human locomotion balance research, we are going to apply obtained with a MoCap system human locomotion data for a humanoid robot balancing. This could be realized by adapt-

ing human gait parameters (joint angles and angular moments, GCOM and ZMP trajectories, etc.) to the robot ones taking into account relevant constraints with kinematic and dynamic corrections.

MoCap systems are usually based on marker/markerless motion capture technologies, using sensors with different physical principles: optical, magnetic, inertial, mechanical, and even acoustic (Field et al., 2009). The most precise technologies are the most expensive, like mechanical exoskeletons with direct joint angles tracking (Wong et al., 2015), inertial sensors (e.g., XSENS system¹) with acceleration and rotational velocity measurements from triaxial accelerometers and gyroscopes (Wong et al., 2015), and optical MoCap based on multi-camera system (e.g., VICON²), which captures 2D videos from several cameras and then merges them into 3D model by triangulation (Field et al., 2009).

In our research we use low cost markerless optical MoCap system based on four depth sensors Kinect 2 and iPi Soft software. We calculate ZMP and GCoM trajectories from human body dynamics and estimate the accumulated errors. Static and dynamic criteria further will be applied for human data re-projection onto human-like gait of Russian biped robot AR-601M, yielding its stable and natural locomotion.

The paper is organized as following. Section 2 describes our system setup, consisting of Kinect-based MoCap system, iPi Mocap Studio software and AR-601M robot. Section 3 considers human body approximation with a single and multiple mass points and introduces two ZMP evaluation methods. Section 4 presents the results of ZMP and GCoM trajectory calculations based on MoCap measurements with accuracy estimation. Finally we conclude and discuss our future research activities.

2 SYSTEM SETUP

2.1 Kinect-based Motion Capture

For human gait registration we use markerless optical MoCap system based on four Kinect 2 sensors, which encapsulate a total area of 23 sq.m with a walking area of 4.5 m length (Fig. 1, 2). Each Kinect sensor contains RGB camera and depth sensor. MoCap system analyzes depth sensor video recordings

¹XSENS is an inertial 3D motion tracking technology based on body-mounted MEMS inertial sensors and multi-sensor data fusion algorithms, www.xsens.com

²VICON is a passive optical motion capture technology based on high resolution multi-camera system and advanced real-time computer vision algorithms, www.vicon.com

to tracks human motion. Next, in order to reproduce human locomotion with a human-like bipedal robot, a human skeleton animation is built and a human 3D model with linear and angular joint motion parameters is reconstructed. MoCap system acquires human motion data in three stages: 1) MoCap calibration; 2) human motion tracking; 3) non-real-time processing with iPi Soft software and MATLAB. These stages were executed with iPi Soft which acquired MoCap data and provided non-real-time processing by merging depth sensor video data from four Kinect sensors, correcting the data and filtering out the noise. Each Kinect sensor was connected to an individual Windows PCs, forming a distributed system with one master PC, which synchronized three other PCs and the corresponding depth sensors' records (Gabbasov et al., 2015).

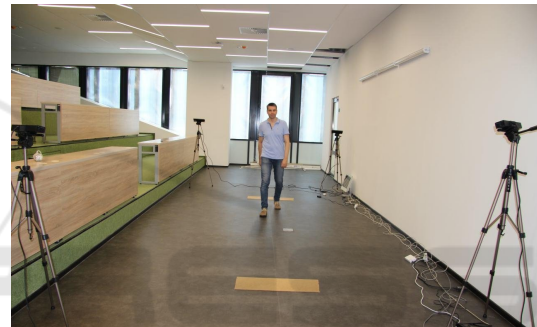


Figure 1: Kinect-based MoCap system: The scene view.

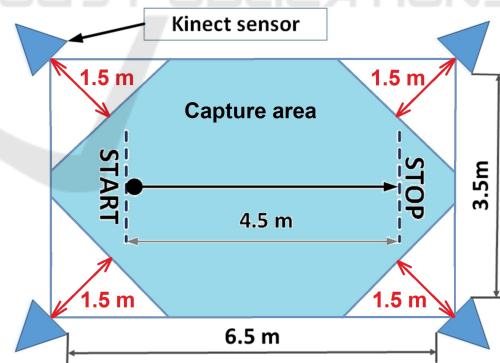


Figure 2: MoCap system: The scene configuration.

The detailed information on MoCap calibration, measurement technique, data acquisition and processing with iPi Soft could be found in (Gabbasov et al., 2015) and iPi Docs resource³. The MoCap calibration evaluates ground position and mutual Kinect sensor localization. During calibration process we had sig-

³iPi Docs: User Guide for Multiple Depth Sensors Configuration, <http://docs.ipisoft.com/User Guide for Multiple Depth Sensors Configuration>.

nificant issue with incorrect definition of a glowing marker position by iPi Mocap Studio which were possibly caused by a weak contrast of the glowing marker relatively to laboratory walls. We have overcome this problem by performing the calibration in the dark room. Unfortunately, such approach increased the average calibration error to 0.045 m (Gabbasov et al., 2015), and thus decreased MoCap measurement accuracy and also impacted the GCoM and ZMP errors.

In our further calculations of human GCoM and ZMP trajectories we use the data which were obtained from iPi Biomech Add-on plugin⁴, such as CoM coordinates and accelerations. We exported biomechanical characteristics into MATLAB and selected a time period where a human walked forward, matching X -axis with forward walking direction and Z -axis with left-hand direction (on default, Y -axis is in upward direction).

2.2 iPi Soft Package

iPi Soft software⁵ uses 3D depth sensors to track human joints and produce 3D animations, providing human pose data with centimeter-level accuracy off-line (Kim et al., 2015). It consists of free iPi Recorder and iPi Mocap Studio software. iPi Recorder acquires depth sensor video data from four Kinect 2 sensors, and then iPi Mocap Studio processes multiple sensor video records off-line, reconstructing 3D model of human locomotion applying inverse kinematics approach. Afterwards we use iPi Biomech Add-on plugin to calculate joint coordinates and angles, linear and angular velocities, accelerations, and CoM positions over time.

Finally, we analyze human gait to identify key features of human locomotion in MATLAB, collecting statistically significant data to create an adequate human gait mathematical model, which could be adapted to AR-601M robot gait mathematical model.

2.3 AR-601M Robot Description

The AR-601M biped robot⁶ (Fig. 3) is a full-size humanoid with the height of 144 cm and weight of 65 kg, having 43 active DoFs (including 12 DoFs in robot legs). Nowadays, robot supports slow locomotion with GCoM trajectory laying within support feet during the its walking (Khusainov et al., 2016).

⁴[http://docs.ipisoft.com/iPi Biomech Add-on](http://docs.ipisoft.com/iPi%20Biomech%20Add-on).

⁵Motion Capture software, supporting markerless technology from Russian company iPi Soft, <http://ipisoft.com>

⁶AR-601M robot is being developed by Russian company Androidnaya Tehnika (Android Technics), <http://en.npo-at.com/products/ar-600>



Figure 3: Android Technics AR-601M robot.

3 MOCAP-BASED HUMAN ZMP CALCULATION

3.1 ZMP from Human Body Dynamics as a Single Mass Point

The biped/human gait is statically stable when the GCoM trajectory lays within a foot support area and the corresponding support polygon (Goswami, 1999), whereas criterion of dynamical stability is described with zero moment point (ZMP) term (Vukobratovic and Borovac, 2004). ZMP of a properly balanced gait coincides with Center of Pressure (CoP), presenting a point under the foot where the ground reaction force fully reduces the effects of forces and moments on the foot from the whole body (Vukobratovic and Borovac, 2004). ZMP is considered as the dynamical equivalent of the GCoM: a body with the ZMP location under the foot is stable, otherwise it is not.

To calculate ZMP from body dynamics as a single mass point we used a rough approximation of biped locomotion by a so-called cart-table model (Kajita et al., 2003), which evaluates ZMP as a function of CoM position and accelerations, anchoring the CoM height (\hat{y}) during locomotion:

$$\begin{cases} x_{zmp}(t) = x_{com}(t) - \frac{\hat{y}}{g} \ddot{x}_{com}(t) \\ z_{zmp}(t) = z_{com}(t) - \frac{\hat{y}}{g} \ddot{z}_{com}(t) \end{cases} \quad (1)$$

where x_{zmp} , z_{zmp} are coordinates of ZMP. We applied equation (1) to the data which were exported into

MATLAB from iPi Biomech Add-on plugin.

3.2 ZMP from Human Body Dynamics as Multiple Mass Points

We represent a human body as a model with a 12 mass points m_i set in the middle of the corresponding body parts (a head, a torso, two shoulders, two forearms, two thighs, two shins and two feet), and human mass distribution for the body parts (Table 1) is performed according to (Haley et al., 1988).

Table 1: Human mass distribution of the body parts (Haley et al., 1988).

Segment	Segment mass
Head	6%
Torso	48%
Shoulder	2.5%
Forearm	2.5%
Thigh	12%
Shin	4.5%
Foot	1.5%

The ZMP equations with multiple mass points via inertia tensor in the sagittal and frontal planes are calculated as follows (Ha and Choi, 2007):

$$\begin{cases} x_{zmp}(t) = \frac{\sum_{i=1}^{12} m_i(\ddot{y}_i+g)x_i - \sum_{i=1}^{12} m_i\ddot{x}_iy_i}{\sum_{i=1}^{12} m_i(\ddot{y}_i+g)} \\ z_{zmp}(t) = \frac{\sum_{i=1}^{12} m_i(\ddot{y}_i+g)z_i - \sum_{i=1}^{12} m_i\ddot{z}_iy_i}{\sum_{i=1}^{12} m_i(\ddot{y}_i+g)} \end{cases} \quad (2)$$

where x_{zmp} , z_{zmp} are coordinates of ZMP and m_i is the point mass of the i -th body part.

3.3 CoM and ZMP Accuracy Estimation Technique

Kinect-based MoCap brings a stochastic error to the true measurement characteristics such as coordinates and accelerations of the i -th body part (Gabbasov et al., 2015) and therefore MoCap-measured values should be treated as a non-stationary stochastic process. We assume that the total measurement error consists of several components: Kinect-based MoCap calibration error (i.e. the error in cross-localization of four Kinect sensors with regard to each other), the accuracy of human motion approximation with iPi Soft, the error in distance estimation between a human body and sensors, etc. Moreover, measurement

error analysis is a quite difficult task because it is impossible to take into account all Kinect sensor configurations and the accuracy of human motion approximation with iPi Soft, which depends on the scene background, human individual anatomical features, clothes' color, etc. Therefore, according to the Central Limit Theorem we can assume that the measurement errors are normally distributed and the variance of the stochastic process is time-independent. Thus, the probability density of the measured values (coordinates and accelerations of the i -th body part's CoM) is defined as:

$$p(x, t) = \frac{1}{\sqrt{2\pi}\sigma} \exp\left(-\frac{(x - \mu(t))^2}{2\sigma^2}\right) \quad (3)$$

where x is a measured value, $\mu(t)$ is a time-dependent mathematical expectation (e.g., a true coordinates or accelerations for a body part's CoM), σ is a variance of the measured value.

In our study, the absolute measurement error could be estimated as a standard deviation from the time-dependent mean. For example, the measurement error of x -coordinate of CoM is computed as the unbiased standard deviation:

$$\Delta x_{com} = \sqrt{\frac{\sum_{i=1}^N (x_i - M(x, t))^2}{(N - 1)}} \quad (4)$$

where $M(x, t)$ is mathematical expectation for x -coordinate of CoM. The mathematical expectation of CoM for i -th body part changes over time along x -coordinate during human locomotion (e.g., foot's CoM acceleration is shown in Fig. 4, blue curve). Therefore we smooth the MoCap-measured data (blue curve in Fig. 4) with moving average to estimate the mathematical expectation (brown curve in Fig. 4).

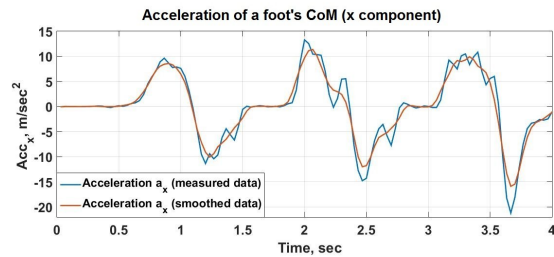


Figure 4: Measured foot's CoM acceleration along the x -axis (blue curve) and its smoothing (brown curve).

We use the same method to calculate the smoothed mathematical expectation of CoM acceleration and coordinates for both human body as a single mass point (the first method, Section 3.1) and all body parts as multiple mass points (the second method, Section 3.2). As far as we provide indirect ZMP measure-

ments, the Error Theory should be applied to calculate ZMP measurement error ΔZMP_x with equation:

$$\Delta ZMP_x = \sqrt{\left(\sum_{i=1}^n \frac{\partial ZMP}{\partial x_i} dx_i\right)^2} \quad (5)$$

where $\frac{\partial ZMP}{\partial x_i}$ is a partial derivative of ZMP function for one of the variables and dx_i is the estimation of absolute measurement error for this variable.

Therefore, the total ZMP error for the first method is calculated as follows:

$$\begin{cases} \Delta ZMP_x = \sqrt{(\Delta x_{com}^2 + (\frac{\hat{y}}{g} \Delta a_{xcom})^2)} \\ \Delta ZMP_z = \sqrt{(\Delta z_{com}^2 + (\frac{\hat{y}}{g} \Delta a_{zcom})^2)} \end{cases} \quad (6)$$

where \hat{y} is average CoM position along the vertical Y-axis.

Whereas the total ZMP error for the second method is calculated as follows:

$$\begin{cases} \Delta ZMP_x = \sqrt{\frac{\sum_{i=1}^{12} (m_i(\ddot{y}_i+g)\Delta x_i)^2 + \sum_{i=1}^{12} (m_i\ddot{x}_i\Delta \ddot{y}_i)^2}{\sum_{i=1}^{12} m_i(\ddot{y}_i+g)x_i - \sum_{i=1}^{12} m_i\ddot{x}_i y_i} + \frac{\sum_{i=1}^{12} (m_i\ddot{y}_i\Delta \ddot{x}_i)^2 + \sum_{i=1}^{12} (m_i\ddot{x}_i\Delta \ddot{y}_i)^2}{\sum_{i=1}^{12} m_i(\ddot{y}_i+g)x_i - \sum_{i=1}^{12} m_i\ddot{x}_i y_i} \sqrt{\frac{\sum_{i=1}^{12} m_i\Delta y_i}{\sum_{i=1}^{12} m_i(\ddot{y}_i+g)}}} \\ \Delta ZMP_z = \sqrt{\frac{\sum_{i=1}^{12} (m_i(\ddot{y}_i+g)\Delta z_i)^2 + \sum_{i=1}^{12} (m_i\ddot{z}_i\Delta \ddot{y}_i)^2}{\sum_{i=1}^{12} m_i(\ddot{y}_i+g)z_i - \sum_{i=1}^{12} m_i\ddot{z}_i y_i} + \frac{\sum_{i=1}^{12} (m_i\ddot{y}_i\Delta \ddot{z}_i)^2 + \sum_{i=1}^{12} (m_i\ddot{z}_i\Delta \ddot{y}_i)^2}{\sum_{i=1}^{12} m_i(\ddot{y}_i+g)z_i - \sum_{i=1}^{12} m_i\ddot{z}_i y_i} \sqrt{\frac{\sum_{i=1}^{12} m_i\Delta y_i}{\sum_{i=1}^{12} m_i(\ddot{y}_i+g)}}} \end{cases} \quad (7)$$

where $x_i, y_i, z_i, \ddot{x}_i, \ddot{y}_i, \ddot{z}_i$ correspond to the coordinates and accelerations of the i -th body part, and $\Delta x_i, \Delta y_i, \Delta z_i, \Delta \ddot{x}_i, \Delta \ddot{y}_i, \Delta \ddot{z}_i$ are absolute error estimations for coordinates and accelerations of the i -th body part.

4 ZMP TRAJECTORY AND ACCURACY ANALYSIS

4.1 ZMP and GCoM Trajectories from Human Body Dynamics

ZMP and GCoM trajectories on the ground plane were calculated from human body data, where human body was approximated a single and multiple

mass points methods, according to equations (1) and (2) correspondingly. Figure 5 represents human ZMP trajectories obtained by a single mass point method (red curve) and multiple mass points method (green curve), whereas blue curve shows the GCoM trajectory and orange ellipses illustrate human footprints. The figure shows that both ZMP and GCoM trajectories are located close to the footprints (and consequently to the corresponding support polygons). It satisfies the static (GCoM) and dynamic (ZMP) stability criteria (Mrozowski et al., 2007) and proves that the human gait was properly balanced. Moreover, the ZMP trajectory which was calculated applying multiple mass point method lays slightly closer to the GCoM trajectory than the calculated with a single mass point method trajectory. As far as both methods process the same MoCap data, it means that they have different accuracy. Only the last segment of ZMP trajectories lays outside the support area (footprint) at the coordinate of 2 m. It emphasizes the balancing changes before a human stop at the end of MoCap walking area.

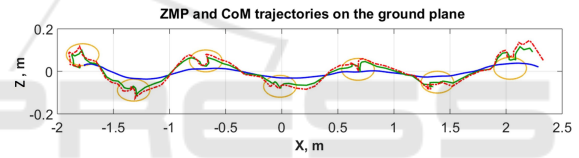


Figure 5: Human ZMP trajectory from single mass point (red curve) and multiple mass points methods (green curve), GCoM trajectory (blue curve) and footprints (orange ellipses) on the ground plane. The X-axis and Z-axis are oriented in the human walking and orthogonal to the walking (lateral) directions respectively.

Figures 6 and 7 show ZMP trajectories vs. time in sagittal and frontal planes respectively which are calculated from human body locomotion dynamics. The significant deviations of ZMP trajectory in the frontal plane in the vicinity of the footprint positions arise from the limitations of MoCap system measurement accuracy.

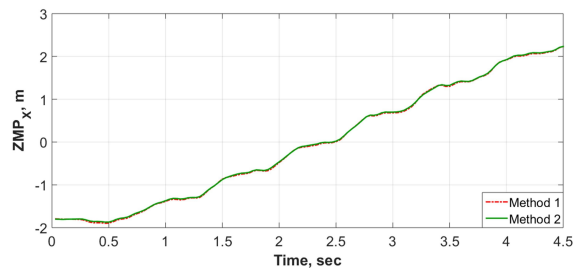


Figure 6: Human ZMP trajectory vs. time in sagittal plane for single mass point (red curve) and multiple mass points methods (green curve).

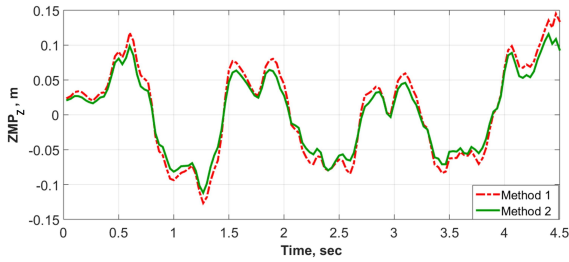


Figure 7: Human ZMP trajectory vs. time in frontal plane for single mass point (red curve) and multiple mass points methods (green curve).

4.2 CoM and ZMP Accuracy Estimation

We estimated the GCoM measurement error as a standard deviation applying equation (4), which gave us the typical values:

$$\begin{cases} \Delta x_{com} \approx 1cm \\ \Delta z_{com} \approx 1cm \end{cases} \quad (8)$$

For the human body model which is built with a single mass point method the total ZMP errors are time-independent due to the model simplicity (Gabbasov et al., 2015), and its values are computed according to equations (6):

$$\begin{cases} \Delta ZMP_x \approx 7cm \\ \Delta ZMP_z \approx 7cm \end{cases} \quad (9)$$

For the 12 mass points human body model the total ZMP errors were calculated according to equations (7). The calculated values of the total ZMP error in the walking direction ΔZMP_x varies from 1 mm to 35 mm (where the value $\Delta ZMP_x = 35$ mm corresponds to the MoCap walking area of 2 m length, i.e. ± 1 m from the center of MoCap scene in Fig. 2), whereas ZMP error in lateral direction ΔZMP_z varies in the range from 1 to 7 mm.

$$\begin{cases} \Delta ZMP_x \approx 3.5cm \\ \Delta ZMP_z \approx 0.7cm \end{cases} \quad (10)$$

Moreover, the ZMP error in the walking direction ΔZMP_x strongly depends on the x -coordinate of ZMP trajectory (i.e., on a human position relatively to the center of Kinect-based MoCap system), which results in the minimal total ZMP error at the center of MoCap walking area and maximal error on the boundaries of the MoCap capture zone. The growth of ΔZMP_x is nonlinear from MoCap capture zone center to its boundaries. While ΔZMP_x was approximately

the same for both ZMP evaluation methods on the boundaries of the ± 1.5 m interval of the MoCap capture zone (centered in the middle of the 4.5 m walking zone), for the MoCap capture zone of 4.5 m (which corresponds to start and stop lines in Fig. 2) the second ZMP evaluation method (Section 3.2) gives much higher total ZMP error ΔZMP_x than the first method (Section 3.1). Therefore, to eliminate the influence of acceleration and deceleration within the first steps and thus to minimize the total ZMP error we restricted the MoCap active capture zone to ± 1 m from the center of the MoCap scene for the second method.

Figures 8 and 9 demonstrate ZMP and GCoM trajectories for the single and multiple mass point methods of human body correspondingly. The total ZMP error is shown with the red bars. The comparison of total ZMP errors for human body models as a single and multiple mass points (equations (9) and (10) correspondingly) demonstrates that the multiple mass point method is more accurate for the shortened MoCap capture zone of 2 m length and could be better applicable to the task of human locomotion analysis by static (GCoM) and dynamic (ZMP) stability criteria of human gait balance.

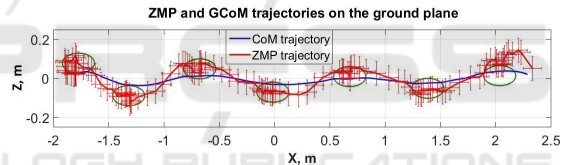


Figure 8: ZMP trajectory (red curve) and the total ZMP errors (red bars), calculated with a single mass point method, and GCoM trajectory (blue curve).

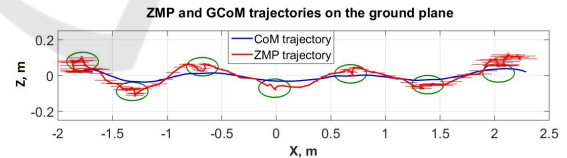


Figure 9: ZMP trajectory (red curve) and the total ZMP errors (red bars), calculated with a multiple mass points method, and GCoM trajectory (blue curve).

5 CONCLUSION AND FUTURE WORK

This paper focused on the analysis of human locomotion. The locomotion data was recorded with MoCap markerless tracking and visualization technology, which is based on four Kinect 2 sensors and non-real-time processing with iPi Soft software and

MATLAB. Human gait balance was analyzed applying static (GCOM) and dynamic (ZMP) stabilities.

Human ZMP and GCoM trajectories were calculated by two methods, which consider human body as a simplified approximation with the models of a single mass point and multiple mass points. Our calculations demonstrated close localization of analyzed GCoM and ZMP trajectories to the human's footprints and the corresponding support polygons. It means that the human walking had static and dynamic stability, proving that the human gait was properly balanced. The comparison of total ZMP errors for human body models as a single and multiple mass points demonstrated that the later method is significantly more accurate for the limited MoCap walking zone of 2 m length (the maximal ZMP error was 3.5 cm along the walking direction and 0.7 cm in lateral direction) than the former one, and thus should be preferred for human gait estimation. Quite significant ZMP trajectory deviations in the vicinity of footprints' positions arise from the limitations of MoCap system measurement accuracy.

Finally, we use MoCap system and analyze human locomotion to identify key features of human walking, collecting statistically significant data to create an adequate human gait mathematical model, which could be adapted to Russian AR-601M robot simulation model, yielding its statically and dynamically stable and more natural locomotion.

ACKNOWLEDGEMENTS

This work was supported by Russian Ministry of Education and Science, and our industrial partner Android Technics under Scientific and Technological Research and Development Program of Russian Federation for 2014-2020 years (research grant RFMEFI60914X0004). Special thanks to iPi Soft company for providing temporary access to iPi Soft Mocap Studio.

REFERENCES

- Asano, F. and Luo, Z.-W. (2008). Energy-efficient and high-speed dynamic biped locomotion based on principle of parametric excitation. *IEEE Transactions on Robotics*, 24(6):1289–1301.
- Chalodhorn, R., Grimes, D. B., Grochow, K., and Rao, R. P. N. (2007). Learning to walk through imitation. In *Proc. of 20th Int. Joint Conference on Artificial Intelligence, IJCAI'07*, pages 2084–2090, San Francisco, CA, USA. Morgan Kaufmann Publishers Inc.
- Dasgupta, A. and Nakamura, Y. (1999). Making feasible walking motion of humanoid robots from human motion capture data. In *IEEE ICRA*, volume 2, pages 1044–1049.
- Field, M., Stirling, D., Naghdy, F., and Pan, Z. (2009). Motion capture in robotics review. In *IEEE Int. Conf. on Control and Automation*, pages 1697–1702.
- Gabbasov, B., Danilov, I., Afanasyev, I., and Magid, E. (2015). Toward a human-like biped robot gait: Biomechanical analysis of human locomotion recorded by kinect-based motion capture system. In *Proc. of 10th Int. Symposium on Mechatronics and its Applications*.
- Goswami, A. (1999). Foot rotation indicator (fri) point: A new gait planning tool to evaluate postural stability of biped robots. In *IEEE ICRA*, pages 47–52.
- Ha, T. and Choi, C.-H. (2007). An effective trajectory generation method for bipedal walking. *Robotics and Autonomous Systems*, 55(10):795–810.
- Haley, J. et al. (1988). Anthropometry and mass distribution for human analogues. In *Military Male Aviators, Volume 1, Aerospace Medical Research Lab., Wright-Patterson AFB Ohio USA, Tech. Rep*, pages 34–38.
- Kajita, S., Kanehiro, F., Kaneko, K., Fujiwara, K., Harada, K., Yokoi, K., and Hirukawa, H. (2003). Biped walking pattern generation by using preview control of zero-moment point. In *IEEE ICRA*, volume 2, pages 1620–1626.
- Khusainov, R., Afanasyev, I., and Magid, E. (2016). Anthropomorphic robot modelling with virtual height inverted pendulum approach in Simulink: step length and robot height influence on walking stability. In *Int. Conf. on Artificial ALife and Robotics (in press)*.
- Kim, H., Lee, S., Lee, D., Choi, S., Ju, J., and Myung, H. (2015). Real-time human pose estimation and gesture recognition from depth images using superpixels and svm classifier. *Sensors*, 15(6):12410–12427.
- Larsen, J. C. and Stoy, K. (2011). Energy efficiency of robot locomotion increases proportional to weight. *Procedia Computer Science, Proc. 2nd European Future Technologies Conference and Exhibition*, 7:228–230.
- Mrozowski, J., Awrejcewicz, J., and Bamberski, P. (2007). Analysis of stability of the human gait. *Journal of theoretical and applied mechanics*, 45:91–98.
- Naksuk, N., Lee, C., and Rietdyk, S. (2005). Whole-body human-to-humanoid motion transfer. In *5th IEEE-RAS Int. Conf. on Humanoid Robots*, pages 104–109.
- Sinnet, R. W., Powell, M. J., Jiang, S., and Ames, A. D. (2011). Compass gait revisited: A human data perspective with extensions to three dimensions. In *Proc. of 50th IEEE Conf. on Decision and Control, and European Control Conf. (CDC-ECC)*, pages 682–689.
- Vukobratovic, M. and Borovac, B. (2004). Zero-moment point thirty five years of its life. *International Journal of Humanoid Robotics*, 1(1):157–173.
- Vukobratovic, M. and Juricic, D. (1969). Contribution to the synthesis of biped gait. In *IEEE Transactions on Biomedical Engineering*, volume 16(1), pages 1–6.
- Wong, C., Zhang, Z.-Q., Lo, B., and Yang, G.-Z. (2015). Wearable sensing for solid biomechanics: A review. *Sensors Journal, IEEE*, 15(5):2747–2760.